FORMATION OF SUPERSATURATED Fe-Li SOLID SOLUTION BY MECHANICAL ALLOYING

Keiichi N. Ishihara, Fumie Kubo, Eiji Yamasue and Hideyuki Okumura

Graduate School of Energy Science, Kyoto University, Sakyo-ku, Kyoto 606-8501, Japan

Abstract. The mechanical alloying of Li with three kinds of Fe powders was performed under various milling conditions. Only in the case of using one kind of Fe powder among three, the formation of Fe-Li supersaturated solid solution was confirmed by X-ray diffraction after 10 h milling. The detailed investigation by Moessbauer spectroscopy and saturation magnetization measurement supports the result. XPS (X-ray photo-electron spectroscopy) measurements were also performed to investigate the surface chemistry of samples. The existence of oxide plays an important role in effective promoting of mechanical alloying in this system.

1. INTRODUCTION

The formation of supersaturated solid solution produced by mechanical alloying (MA) has been reported for various systems [1,2] such as Fe-Cu, Fe-Ag, Ag-Cu and Co-Cu. Among them, the iron systems are of importance due to their prospects for application as well as scientific interests. Since the bcc iron is ferromagnetic, the process of atomic mixing during milling can be monitored by the measurement of magnetic properties such as saturation magnetization and Moessbauer spectroscopy [3].

It is known that lithium (Li) is the only element that reacts with nitrogen gas at ambient temperature and under ambient pressure. In order to enhance the properties, MA of Li with some elements has been performed by our group [4,5]. In this work, MA of Fe-Li alloy was performed to investigate the possibility of forming a supersaturated solid solution, where the Fe-Li system is completely immiscible in both solid and liquid states.

2. EXPERIMENTAL PROCEDURE

MA of fragmented Li (98% purity) with three kinds of iron powders, shown in Table 1, was performed using a high energy vibrating ball mill with water jacket (Nisshin Giken, Super Misuni NEV-MA8) under argon atmosphere. No process control agent was used. The vessel and balls were made of stainless steel. The lattice parameter was measured using Fe (211) plane by X-ray difractometry (Rigaku RINT2000) with internal Si standard under argon atmosphere. Chemical analyses of sample were performed by ICP (Inductive Coupled Plasma) emission spectrometer. The surface chemistry of the sample was analyzed using XPS (X-ray photo-electron spectroscopy), where MgK_α (1253.6eV) was used as X-ray anode under ultra high vacuum. The ^{57}Fe absorption Moessbauer spectroscopy and VSM (vibrating sample magnetometery) were performed to study the magnetic properties of iron atoms in samples.

3. RESULTS AND DISCUSSIONS

3.1. MA of Li with three kinds of Fe powders

The MA of Li with three kinds of iron powders was performed in the conditions shown in Table 2. The atomic ratio of Li in the initial sample was kept at

Corresponding author: Keiichi N. Ishihara, e-mail: ishiahra@energy.kyoto-u.ac.jp@

Table 1. Characteristics of three kinds of iron powders.

Label	Average diameter	Oxygen contents (wt.%)	Nitrogen contents (wt.%)
Fe(a)	4 μm	0.38	1.47
Fe(b)	53 μm	1.46	0.0061
Fe(c)	150 μm	0.04	0.0015

Table 2. Milling conditions and the results of milling.

No.	Fe powders	Ball to powder ratio	Sample weights (g)	Recovered sample weight ratio after 10 h milling	Li content in powder sample after 10 h milling
1	Fe(a)	10 to 1	10	40%	-
2	Fe(a)	10 to 1	5	50%	-
3	Fe(a)	20 to 1	5	70%	14 at.%
4	Fe(b)	10 to 1	10	100%	15.3 at.%
5	Fe(c)	10 to 1	10	none	-
6	Fe(c)	10 to 1	5	20%	-
7	Fe(c)	10 to 1	2.5	20%	-
8	Fe(c)	20 to 1	5	20%	-
9	Fe(c)	40 to 1	2.5	50%	10.5 at.%
10	Fe(c)	60 to 1	2.5	70%	-

Table 3. Moessbauer parameters of decomposed spectra. IS, QS and IF means isomer shift, quadrupole splitting and internal field, respectively.

Partial	FWHM(mm/s)	Area(%)	*IS* (mm/s)	*QS* (mm/s)	*IF*(T)
1	0.37	60.0	0.00	0.013	2.85
2	0.58	35.6	0.01	0.023	0.83
3	0.86	4.4	0.10	1.42	
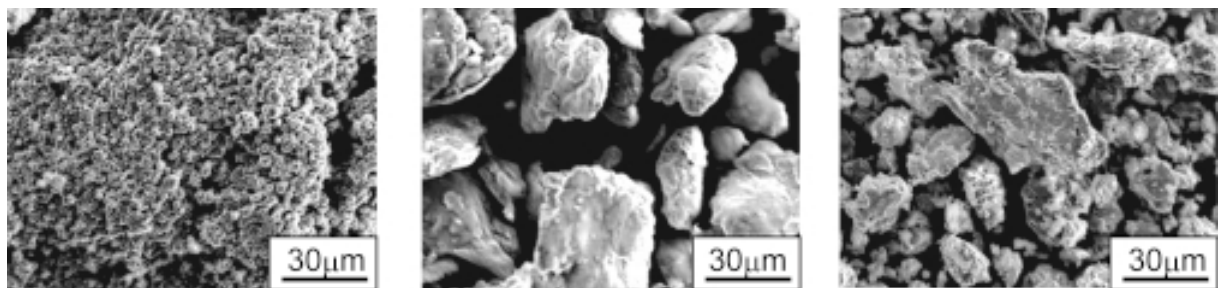
Fig. 1. SEM images of powder samples after 10 h of milling for Fe(a)-Li (No.3), Fe(b)-Li (No.4) and Fe(c)-Li (No.9).

15.3 at.%. In the case of Fe (a) (No.1), 40 wt.% of input materials was recovered as a powder form after 10h milling and the remaining 60% adhered to the vessel and ball surface. In the case of Fe (b) (No.4), 100% of sample was recovered as a powder form after 10 h milling. For Fe(c) (No.5), no

powder sample was recovered and the vessel and balls were coated with the sample showing a metallic surface. In order to improve the recovery yield, the sample amounts were reduced and the ball-to-powder ratio was increased. The results are shown in Table 2.

The chemical analyses of powder samples after 10h milling for No.3, 4, and 9 were performed. The lithium contents in the powder samples are also shown in Table 2. Since lithium adheres to the vessel and balls much more than iron, the Li contents in powder sample for No.3 and 9 are decreased. The 2 wt.% of Cr and 1 wt.% of Ni were detected as contamination from stainless steel vessel and balls for sample No.9. For samples No.3 and 4, the contamination from container was relatively small. The SEM images of these samples are shown in Fig. 1. In the case of No.3, the powder is agglomerated. For No. 9, the size of powders is not homogeneous compared to the other two samples. The adhered samples are detached from the surfaces during milling to form larger particles.

3.2. Analyses of milling process for Fe(b)-Li (No.4)

The MA processes for the sample No.4 have been investigated in details. The X-ray diffraction profiles up to 50 h milling are shown in Fig. 2. It is noted that a small amount of iron oxide is seen in the case of initial sample and $LiFeO_2$ and LiOH are seen for 1, 5, and 10 h milling. Since the LiOH is the product of the reaction of Li_2O with water in air during the handling, it indicates the existence of Li_2O.

Fig. 3 shows the change of lattice parameter of the sample, compared with that of pure iron, (Fe(b)) as a function of milling time. MA samples of pure iron were produced in the same conditions as those for sample No.4. The lattice parameters for the Fe(b) and Fe(b)-Li powder increase with milling time (> 10 h) and the values for Fe(b)-Li are longer than those for the pure iron. The increase of lattice parameters for mechanically milled pure iron is attributed to severe deformation [6,7]. Thus, the Fe-Li sample forms a solid solution, although these elements are thermodynamically immiscible in the solid and even in the liquid state. The lattice parameter of supersaturated solid solution was expressed by thermodynamical parameters [8]. Using this expression, the Li content in supersaturated solid solution for the 50-h-milled sample can be estimated as 1.1 at.% Li. The lattice parameters
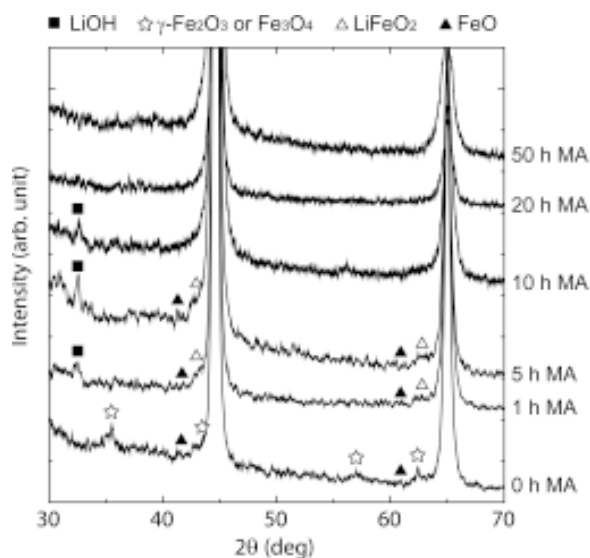

Fig. 2. X-ray diffraction profiles up to 50 h of milling for Fe(b)-Li.
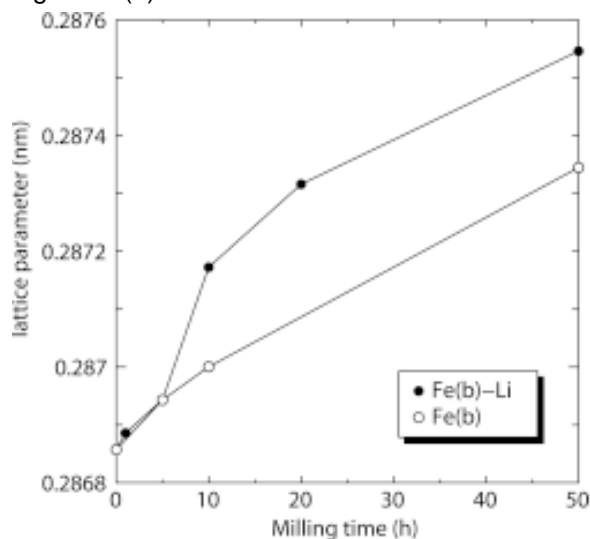

Fig. 3. Changes of lattice parameter of Fe(b)-Li and Fe(b) as a function of milling time.
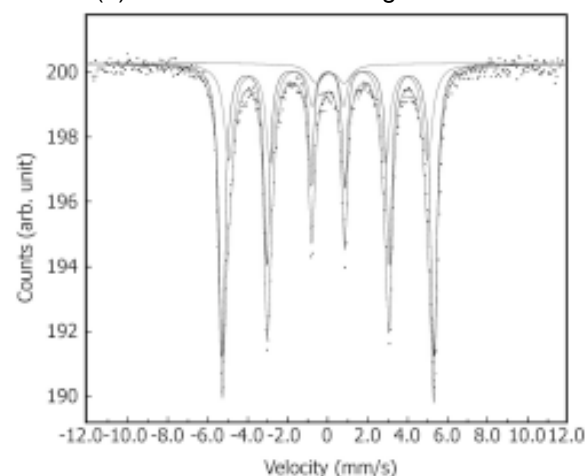

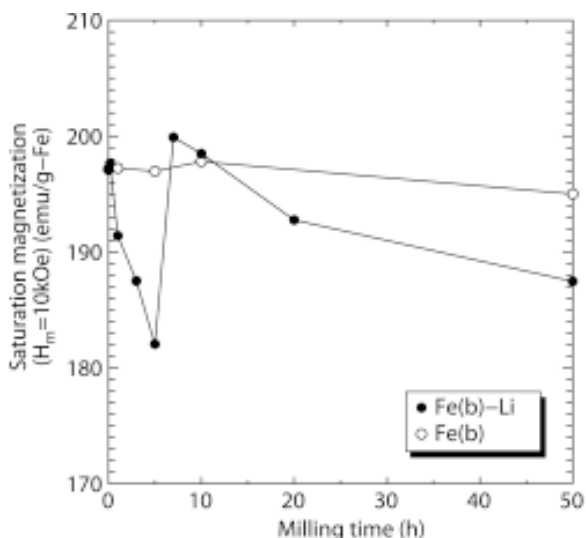**Fig. 4.** ^{57}Fe absorption Moessbauer spectra for Fe(b)-Li after 50 h of milling.

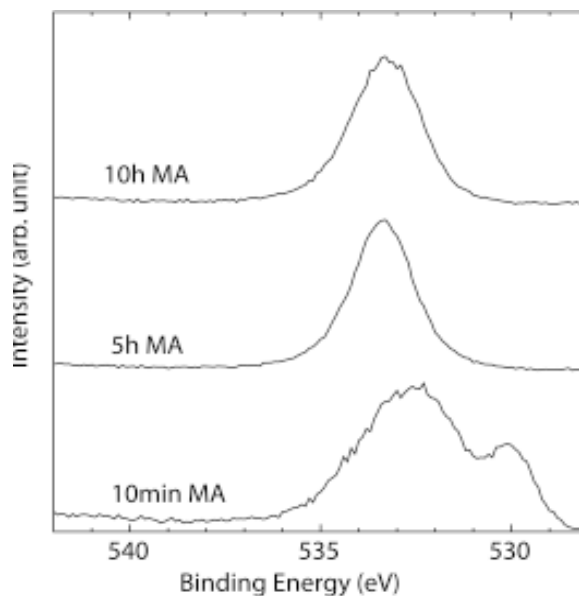**Fig. 5.** Saturation magnetization for milled Fe(b)-Li and Fe(b).

Fig. 6. O (1s) XPS spectra for Fe(b)-Li.

for the other two samples (No.3 and 9) do not show such increase.

[57]Fe absorption Moessbauer spectra for 50-h-milled sample are shown in Fig. 4. The spectrum can be decomposed into three components. The existence of Fe atoms that have a smaller hyperfine magnetic field compared with pure Fe can be clearly seen, indicating formation of supersaturated solid solution. The specific parameters of these components are shown in Table 3. The result indicates that about 40% of iron atoms exist in the smaller hyperfine magnetic field.

These results show the formation of the supersaturated solid solution in the Fe-Li system. Furthermore, it is noted that milling using Fe (b) is the most effective among the three powders. In order to investigate the process during milling, the magnetizations of these samples were measured by using VSM. The magnetization at H=10kOe, which is appropriately assumed to be the saturation magnetization of iron in each sample, is plotted with milling time and shown in Fig. 5. In the case of Fe(b) sample, the magnetic moment decreases slightly during milling, which is attributed to the lattice expansion by the severe deformation as seen in the lattice parameter increase. The decrease of magnetic moment at early stage of MA is attributable to the formation of FeO or LiFeO (both are

paramagnetic) as a result of the reduction by lithium of the ferrimagnetic Fe_3O_4 layer that covers the surface of the pure iron core. Further milling should thus promote the reductive reaction of Fe(b) powder to newly produced pure iron near the powder surface, resulting in the increase of the saturation magnetization after 7 h milling. It should then be followed by the gradual formation of the supersaturated solid solution, reducing the sample magnetization. The events explained above are consistent with the X-ray results. The reaction of iron oxide and lithium was also confirmed by XPS measurements as shown in Fig. 6. In the case of 10 min milling sample, the peak of iron oxide [9,10] around 530 eV, which disappeared after 5h milling, was clearly observed. The peaks around 533 eV correspond to LiOH [11], which can be produced by exposing Li_2O in the ambient atmosphere, which indicates also that the iron oxide reacted with lithium during MA.

The results above can explain the reason why use of the Fe(b) powder, which has higher concentration of oxygen than others (Table 1), leads to the effective MA. The hard iron oxide on the surface of iron powder promotes the pulverization of both iron and lithium powders at early stage of milling. Then, iron oxide reacts with lithium when they contact with each other. After that, the hard lithium

oxide promotes the mixing of the sample. Consequently, the supersaturated solid solution was produced. The oxide film thus plays an important role for the microstructural modification during MA process.

4. CONCLUSIONS

The MA of Li with three kinds of Fe powders was investigated. It has been concluded that the Fe-Li supersaturated solid solution can be produced by MA process and that the existence of oxide as impurity plays an important role for promoting MA in this system.

REFERENCES

[1] C. Suryanarayana // *Prog. Mater.* **46** (2001) 1.
[2] E. Ma // *Prog. Mater. Sci.* **50** (2005) 413.
[3] J. Kuyama, H. Inui, S. Imaoka, S. Nasu, K. N. Ishihara and P. H. Shingu // *Jpn. J. Appl. Phys*. **30** (1991) 854.
[4] K.N. Ishihara, K. Shichi, F. Kubo, K. Irie, E. Yamasue and H. Okumura // *J. Alloy and Comp*, in press.
[5] K.N. Ishihara, K. Irie, F. Kubo, E. Yamasue and H. Okumura // *Mater. Sci. Eng. A* (2006), doi:10.1016/j.msea.2006.02.273.
[6] S. Ram and H. J. Fecht // *Materials Transactions, JIM* **41** (2000) 754.
[7] H. Moumeni, S. Alleg and J.M. Greneche // *J. Alloy and Comp.* **386** (2005) 12.
[8] K. N. Ishihara, In: *Non-Equilibrium Processing of Materials*, ed. by C. Suryanarayana (Pergamon, Amsterdam, 1999), p. 5.
[9] C. R. Brundle, T. J. Chuang and K. Wandelt // *Surf. Sci.* **68** (1977) 459.
[10] T. Fujii, F. M. F. de Groot, G. A. Sawatzky, F. C. Voogt, T. Hibma and K. Okada // *Phys Rev. B* **59** (1999) 3195.
[11] I. Ismail, A. Noda, A. Nishimoto and M. Watanabe // *Electrochimica Acta* **46** (2001) 1595.